

# A Low-Cost, Clutter-Cancelling Life Detection System for First Response after Natural Disasters

Sachin Konan

## Abstract

Earthquakes are devastating natural phenomena which affect regions across the world. The recent Japan earthquake of 2016 or the memorable Nepal Earthquake of 2015 each claimed hundreds of lives, whereby a majority died buried under material before first-response excavation. In order to expedite the first-response procedure and save lives of victims, a low-cost system was sought to be engineered. Discovering the primary means of life were physical movements of the heart and chest, an elementary prototype with an off-the-shelf Doppler radar was built last year to detect the oscillating heart and chest movements of humans, which ultimately failed during through-wall tests behind denser, larger barriers because of the auxiliary signal: clutter. Clutter was the portion of signal that reflected off the frontal area of the barrier and traveled directly to the receive antenna; in through-wall applications clutter is the strongest receive signal, causing over-saturation and decreased sensitivity to lower amplitude/frequency signals. Therefore, an innovative clutter cancellation system was designed which operates off the principles of destructive interference, finding the optimal phase and amplitude characteristics of a cancellation signal which can completely cancel the clutter. The new radar, which operates at S-Band, is followed by a cascade of amplifiers and filters and is processed with a Python Script, which down-samples, splits, filters, selects, and transforms a large time-based data-set to a frequency spectrum. The system was tested on human subjects behind 2m. of plaster, 1m. concrete, and 1.47m. of brick wall over three trials. Each trial yielded outstanding results which showed signs of heartbeats and respiration on-par with those predicted by medical literature, proving the system's field application. It was noted that the ratio of these vital signals to noise was constant across materials, strongly suggesting the radar is capable of detection through even larger material. Although the radar met initial design constraints, an expensive price-tag procured the development of a printed circuit board version, which is currently in development. Future work lies with testing through larger materials such as boulders and developing a real-time cancellation algorithm.

## Acknowledgments

1. I profusely thank Professor James Aberle of Arizona State University for his invaluable help throughout the course of the project, providing advice on the electrical engineering and RF Design portions of the project during our weekly Skype Calls and opening the door to testing RF components at the ASU Connection One Laboratory.
2. I would also like to thank Raveesh Magod and Mahdi Javidahmadabadi for teaching me how to use the high-frequency oscilloscope and spectrum analyzers at the laboratory, respectively, giving me the opportunity to test the radar on my own schedule.

# Contents

<b>1</b>	<b>Introduction</b>	<b>4</b>
<b>2</b>	<b>Alternate Solutions</b>	<b>5</b>
<b>3</b>	<b>Background</b>	<b>6</b>
<b>4</b>	<b>Electrical Design</b>	<b>9</b>
4.1	RF Design . . . . .	9
4.1.1	First Radar Prototype . . . . .	9
4.1.2	Clutter-Cancelling Radar . . . . .	10
4.2	Filter and Amplifiers . . . . .	11
<b>5</b>	<b>Signal Processing</b>	<b>12</b>
5.1	Clutter Cancellation . . . . .	12
5.2	Decimation . . . . .	15
5.3	Sliding Hanning Window Buffer . . . . .	15
5.4	Filter . . . . .	15
5.5	SNR Estimation Algorithm . . . . .	16
5.6	Fast Fourier Transform . . . . .	18
<b>6</b>	<b>Results</b>	<b>18</b>
6.1	Methodology . . . . .	18
6.1.1	Plaster Wall . . . . .	19
6.1.2	Brick Wall . . . . .	20
6.1.3	Concrete Wall . . . . .	21
6.2	Analysis of Results . . . . .	22
<b>7</b>	<b>Conclusion</b>	<b>23</b>
<b>8</b>	<b>Implementation</b>	<b>24</b>
<b>9</b>	<b>Future Research</b>	<b>25</b>

## 1 Introduction

Earthquakes are devastating natural disasters which affect regions all around the world. There are about 15,000 earthquakes each year, with about 150 of these with magnitude 6 or higher on the Richter scale [3]. Earthquakes can destroy vast amounts of infrastructure that can bury citizens under piles of rubble. This can make it extremely difficult for a first-response team to find the location of a buried victim.



Figure 1: Collapsed Building

Victims that are buried under rubble have limited life-cycle. Without an oxygen supply, death is imminent within a couple of hours. With an oxygen supply the average life span is 3-7 days [3]. The main cause of death is a condition known as Crush Syndrome. With victims under tons of material for long periods of time, human tissue starts to compress, and blood circulation slowly ceases to a stop. Cells must undergo anaerobic respiration which produces lactic acid. Prolonged exposure to lactic acid causes the membranes of cells to rupture and release toxic chemicals into a specific area of the body. However, once a victim is recovered all the pressure goes away, and these toxic chemicals are transferred throughout the body through blood circulation. The life-threatening form of Crush Syndrome forms after continuous pressure from more than two days. Another cause

of death is Carbon Dioxide Suffocation and Heat Stroke. Being confined to a solitary space for a large period can suffocate the victim because carbon dioxide can diffuse out of the closed space. For these reasons, the Nepal Earthquake killed 8,617 and injured 16,608 victims. The man in Figure 1 [15] was found over thirteen hours entombed in rubble.

Emergency Response Teams (ERT) will excavate the most-populated areas of the devastated city first, such as suburban areas, schools, malls, and churches. From there on, discovery depends on interaction with locals. A system must be designed that can be sent remotely to expedite the first-response process. This devise could be sent into specific areas specified by the ERT to collect data from specific locations, while the ERT searches the most populated areas. This would decrease the time to recovery and rate of death to Crush Syndrome.

## 2 Alternate Solutions

The four main indicators of life include: respiration, heart-rate, electric potential pulses, and the body temperature. The first method of detection that was investigated was electric potential pulses, initially inspired by the sensors in the bills of platypus. Platypuses have a “6th sense” known as their electroreception sense. In the dark murky waters of Australia, platypuses cannot find their prey using visual cues. For this reason, the platypus utilizes its electroreception sense to detect the oscillating electric fields generated by muscle contractions of the moving prey as seen in Figure 2 [13].

This astounding feat of nature was investigated as means of life detection, although was eliminated due to the sensitivity and price of such a sensor.

Non-Contact methods for heart-beat observation have been studied for the past decade and are quite successful at estimating the heart-beat and respiration rates of humans and animals through air for hospital applications. These devices use Doppler RADAR to record the oscillating movements of the chest and heart [6]. The chest/heart motions have very small displacements, making them difficult to detect in open-air, let alone degraded environments. In fact, significant front-end architecture was developed to extract heartbeat and respiration signals through several feet of pure air[12]. However, an un-documented application of Doppler radar’s is with through wall scenarios, whereby Signal Processing and Electrical Architecture must be designed to find the

minute movements of vital signs among the very noisy signal. Medical literature states that the Doppler shift from the respiration and heartbeat should range from 0.1–0.8 Hz and 0.8–2 Hz, respectively [5].

### 3 Background

RADAR works by sending out low-power radiation at a target in hopes of determining either range or velocity [7].

There are two varieties:

1. Chirp RADAR – Sends out a series of pulses of radiation and is used to determine the range of a target by measuring the time delay from transmission to reception
2. FMCW RADAR- Frequency Modulated Continuous Wave RADAR sends out a continuous sinusoidal wave, and can be used to measure range and velocity.

Doppler RADAR is a type of FMCW RADAR.

Last year, a low-cost Doppler radar module was used called the HB-100. The HB-100 sends out an X-Band, 10.525 Ghz signal, through wall, where it was received and amplified/filtered through a series of filters. Afterwards a MUSIC Algorithm was used to reveal the frequency content within the signal. The radar was capable of detecting humans through two feet of cinder-block wall, but struggled to detect through more dense materials such as concrete or brick. [12].

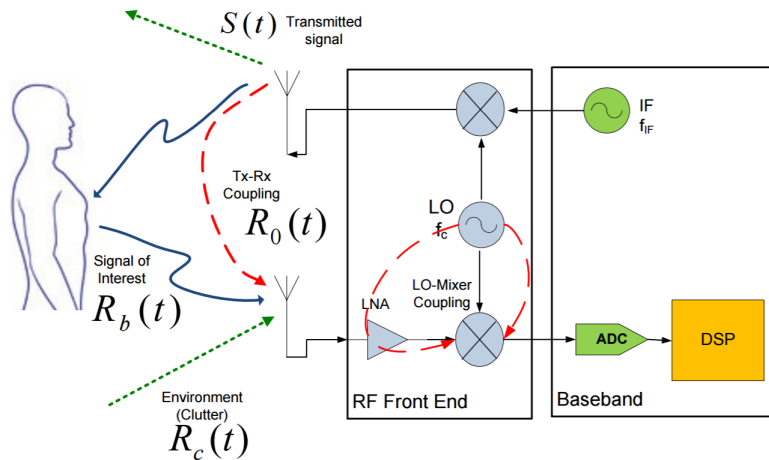


Figure 2: Clutter Signal [9]

The reason for this was the presence of two signals called clutter and transmit-to-receive leakage.

Figure 4 shows that the transmit wave ( $S(t)$ ) partially goes to the human and is observed in the receive path as ( $R_{ab}(t)$ ). Additionally, in that receive path, there exists two additional signals -  $R_{c,t}$  and  $R_{o,t}$  - which represent the transmit to receive coupling and clutter respectively. Transmit to receive coupling is the portion of signal which "leaks" from the transmit antenna to the receive antenna and is a major problem issue for dual antennas that are closely-spaced. Clutter is the largest portion of signal in the receive path and is caused by the immense transmit signal reflections off the frontal barrier of the material looking to be penetrated. Every material has different permittivity constants, represented by  $\epsilon_0$ . The permittivity constants of different materials, not only affect how much signal passes through the material, but also how much is reflected off its frontal area, therefore contributing to clutter. Materials such as concrete or brick have extremely low permittivities, so clutter is an evident problem. However, a unique characteristic of this signal is that as long as no auxiliary movement is introduced into this system, the phase and amplitude characteristics are constant, presenting the possibility of complete cancellation, which will be addressed later on.

Moreover, the reason these prevalent signals effect the radar's detection performance is because of over-saturation at the receive end of the radar. With the largest percentage of signal being the clutter, then leakage, then Doppler signal, the receive antenna can often times over-saturate with auxiliary data. Clutter's amplitude can be tens of folds greater than that of the Doppler data. When received by the RX Antenna, the signal then goes through a Low-Noise Amplifier, where if the Doppler radar signal is too small, then it will be completely overshadowed by the higher frequency, amplitude signals. Additionally, the noise figure of these amplifiers, which in the 2017 radar's implementation, was nearly 0.56 dB, which is extremely high in comparison to the amplitude of the vital signal. Therefore, with the combined effects of clutter and the inherent noise characteristics of amplifiers, detection of human life through material with classical radar configurations is nearly impossible.

Previous works with clutter cancellation lie with satellite and cellular communication. These applications use variable attenuators and phase modulators to adjust the phase and amplitude characteristics of a cancellation wave until it is one hundred eighty degrees out of phase with the clutter signal, at which point the cancellation signal is added to the clutter to achieve minimal clutter presence. These approaches have used expensive phase/amplitude detectors to monitor the "level" of cancellation insinuated by varying changes. In this implementation, similar circuitry shall

be implemented; however, the cancellation path must be vastly simplified by fewer components to reduce cost and overall complexity of the analog front-end.

The second issue is noise. There are two major manifestations of noise in this scenario: phase-noise and amplifier noise [9]. Phase-noise is found in the voltage controlled oscillator, where "hiccupps" in the oscillation creates irregularities in phase. Because Doppler RADAR uses a homo-dyne receiver where the transmit signal is mixed with the received signal, phase noise does not effect close range applications. The flight time delay is nanoseconds, so the phase-noise is MHz away from the carrier - a negligible value [4]. Amplifier noise is generated from the Low Noise Amplifier in the RF circuit and from the Operational Amplifiers in the amplifier/filter circuit. Research into creating a Doppler RADAR for non-contact vital estimation through Doppler RADAR, used a series of steps in signal processing to minimize the noise.

Ultimately, even if a radar addresses these concerns, the attenuation factors faced by dense materials on radiation can never be subdued. The permittivity constants of various housing materials were desired, so researchers found the attenuation factors per foot [8] of each material: concrete (-20 dB/foot), brick (-16 dB/foot), cinder-blocks (-15 dB/foot), plaster (-7 dB/foot). Since antennas generally have a maximum loss of -30 dB and under the assumption that the minimum amplitude of detected signal is -120 dB, the radar must have power outputs on the range of 20 - 30 dB at S-Band.

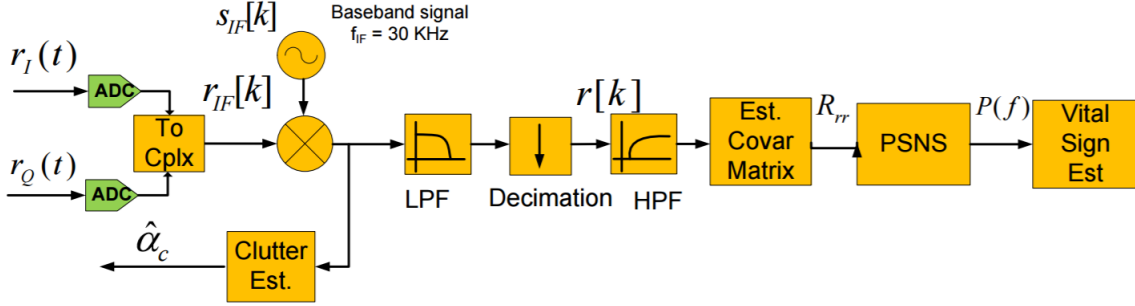


Figure 3: Digital Signal Processing Chain [9]]

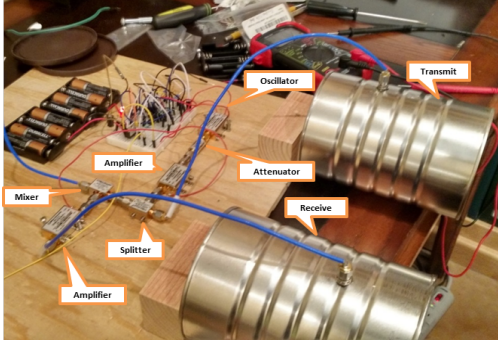
A "sliding Blackman-Harris window" buffer was used to break up the large signal into smaller portions[9]. Then a MUSIC algorithm was used to accurately determine the prevalence of the heartbeat and respiration signals. These methods helped reduce noise in their final calculation, so the steps were adopted in this research. However, the issue with MUSIC is that in order to

reject noise, the number of signals must be known in advance. This unorthodox approach to noise rejection vastly improved the signal to noise ratio of the resulting system, this allowing the team to accurately measure the vital signals of medical patients from as far as 3 m. away. The filtering techniques used by these researchers will be modified and adapted in this research.

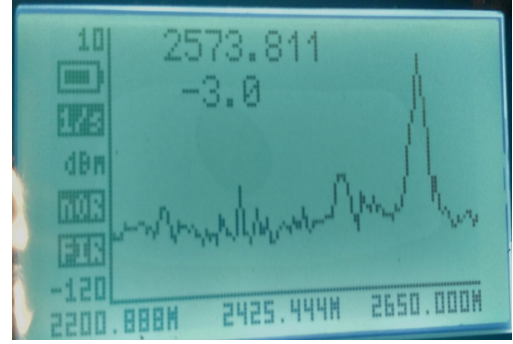
## 4 Electrical Design

### 4.1 RF Design

#### 4.1.1 First Radar Prototype



(a) Old radar [2]



(b) RF Explorer Data [2]

Figure 4: 2016 Radar Prototype

The first version of the redesigned, 2.7 GHz radar system used an orthodox schematic, with a voltage controlled oscillator, a power amplifier, a splitter, a frequency mixer, and a low noise amplifier.

The radar used custom-made coffee-can antennas to transmit and receive signal. Additionally, a low-cost power supply was built to support the power-hungry RF electronics. While this radar was much better equipped to locate life through wall and rubble because of its lower operating frequency and larger power output, it failed in the same respect with the previous radar in that clutter dominated the output of the radar. This hypothesis was confirmed by connecting the radar's receive antenna to a spectrum analyzer to analyze the signals found in the receiver. As seen in Figure 5b, the radar's antenna has a strong peak at the carrier wave, which is around 2.6 GHz, but is surrounded by one strong peak, which is the clutter signal. In response to this test, a clutter cancellation circuit was devised to remove this detrimental signal. The first approach stemmed from

audio-cancellation, which uses sensors to measure the level and frequency of sound of a surrounding room to generate an anti-wave that destructively interferes with noise to generate silence. The idea was adopted, although the device that would be modulating the phase and amplitude characteristics of the radar's cancellation wave is a vector modulator.

#### 4.1.2 Clutter-Cancelling Radar

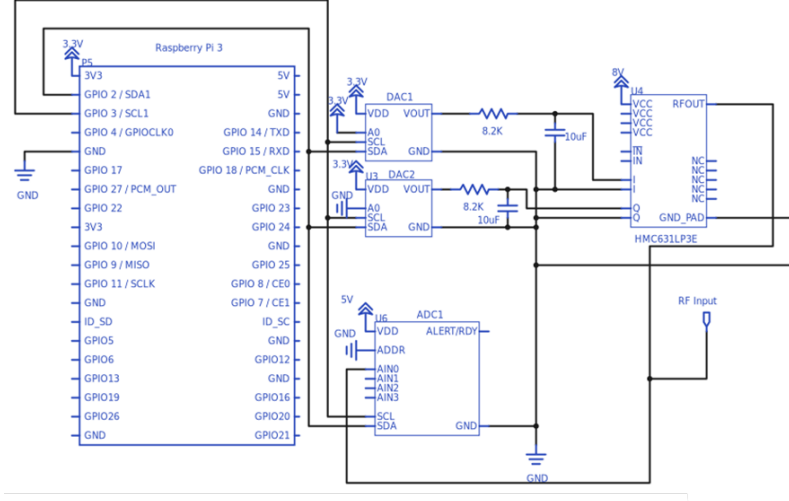


Figure 5: Raspberry PI with DACS [2]

This Cancellation system consists of the same components as the first prototype radar, however a second splitter was used to "sap" some of the transmitted signal and feed it to a vector modulator, where there were two digital input pins which could be configured to adjust the phase and amplitude characteristics of the output wave. Afterwards, the modulated cancellation signal was added to the received Doppler + clutter signal, where in the case of perfect cancellation, only the Doppler signal would remain. These pins were controlled with two digital-to-analog converter chips, called the MCP 4725. These chips were configured with a pocket-sized computer called the Raspberry PI, which through an i2c communication port, was able to digitally compute a given phase and amplitude setting and change the voltage outputs of the two DAC's accordingly. The conversion between a physical phase and amplitude setting and digital input voltage for the vector modulator was governed by two equations.

I Voltage or Phase Control:

$$V_i = 1.5 + \frac{fixed_{gain}}{max_{gain}} * \cos(\theta)$$

Q Voltage or Amplitude Control:

$$V_q = 1.5 + \frac{control_{gain}}{max_{gain}} * \cos(\theta(fixed))$$

Once a certain or amplitude value is changed it is mixed with the sent, carrier wave and observed with an analog-to-digital converter chip called the ADS1115. This chip is capable of sampling up to 800 samples per second, and was run on a separate Python thread to increase processing time during testing. This chip was also connected via i2c with the DAC's. With these chips the entire clutter cancellation system is analogous to a control system, which continuously makes changes, records its effects, and makes new changes accordingly.

## 4.2 Filter and Amplifiers

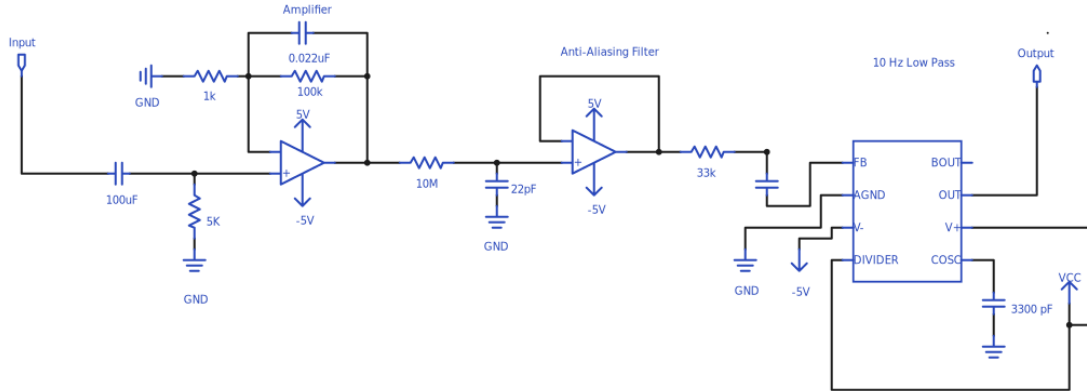


Figure 6: Analog Circuit [2]

The first stage of the circuit is an amplifier that allows the ADS 1115 to recognize a change in voltage in the RADAR. This 40 dB amplifier acts as an active band pass filter that has a bandwidth ranging from 1 to 30 Hz. The second stage of the circuit is a physical Anti-Aliasing low-pass filter that limits the signal to a range that will display heartbeat and respiration. The filter, along with the amplifier, can be seen below. The values of R2 and C2 were determined using the equations

below [1]. This element is a vital part of the circuit, because the ADS 1115 has a max sampling rate of 800, and if any frequencies greater than that pass into the signal, it may distort the heartbeat and respiration signals. Afterwards, the signal passes through a 5th Order 10 Hz Low Pass filter. The first stage is a simple, passive 10 Hz low pass filter which was calculated using the equations below. However, the LTC 1062 Chip used has a tunable clock frequency, controlled by the end capacitor, that determines the order of the passive filter. In this case, a 3300 pF was used to attain a 5th order response, but can be tuned for even greater steepness with larger capacitor values.

$$V_g = \frac{R_2}{R_1} = 40 \quad (1)$$

$$30Hz = \frac{1}{2 \times \pi \times R_1 \times C_1} \quad (2)$$

$$10Hz = \frac{1}{2 \times \pi \times R_2 \times C_2} \quad (3)$$

## 5 Signal Processing

After the signal has been collected from the ADS 1115, the Raspberry Pi runs the data through a series of algorithms that are all written in Python:

1. Clutter Cancellation
2. Sliding and Hanning Window
3. Filter
4. Novel Eigen-Based SNR Selection
5. FFT

### 5.1 Clutter Cancellation

While previous attempts at clutter cancellation have used phase detectors and amplitude detectors to measure clutter's phase and amplitude, those solutions are extremely expensive. However, through Python simulation it was observed that during cancellation with the clutter and cancellation signal, the DC offset at the mixer was closest to zero. This is a factor of the multiplicative and additive properties of sin waves, where when one wave is added to another, one gets another sin wave. That means when one multiplies the two terms, the amplitude of the RF wave will be

represented by the DC offset of the sin wave produced at the output of the mixer. Additionally in Figure 7, the radar was initially in front of a wall, but when antennas were repositioned to open-air, the signal instantly dropped, indicating that clutter has a strong relation to the DC-offset of the output signal.

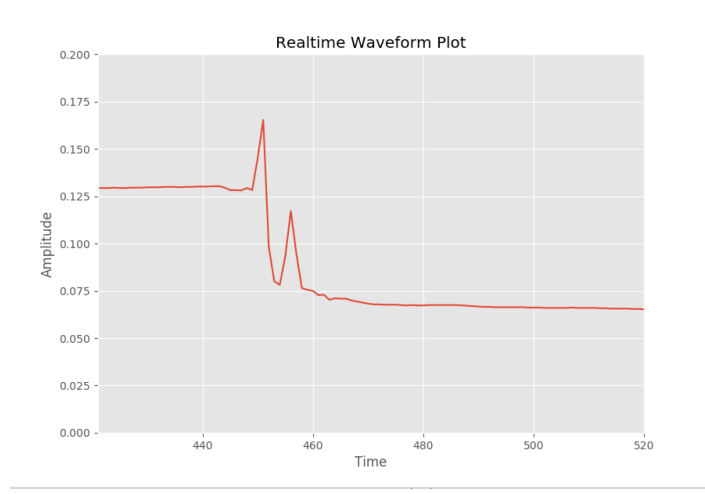


Figure 7: Evidence of DC-Offset [2]

With this observation, a calibration program was devised that could run at the beginning of each radar test. The first investigated method was the most simplistic approach, which was a program that would search through a sparse matrix of phase and amplitude values, find which coordinate had the smallest output voltage, and search a finer grid around that point (Illustrated in Figure 8b). The resultant graph was that of a 3D sinusoid, and the valley's of that graph were the points at which the cancellation signal were 180 degrees out of phase with the clutter signal and of same amplitude.

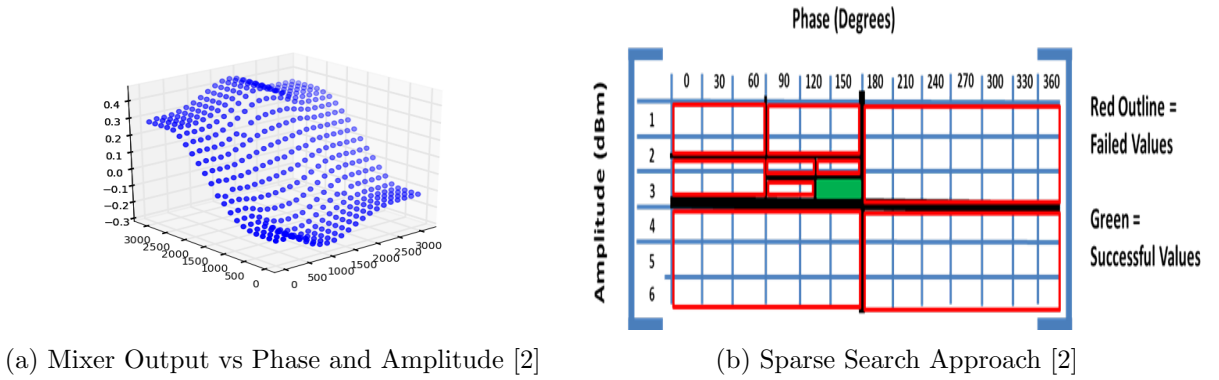


Figure 8: 2D Sparse Search

While this technique succeeded in its relatively short operating time and consistent results, it failed in that having a sparse search as the first stage of a increasingly specific search allowed for unseen valley's to be disregarded. For example the first search went through an 8 by 8 matrix concentrated between values of 0 and 4096. However, say if a valley were seen in a junction between theses points, then the program would falsely keep searching for another peak. This bug could be fixed with every-growing data points within the first search, but eventually the act of doing so took away from searches "sparsity".

In the next approach, a series of one dimensional searches were used to vastly simplify this complex puzzle. First, the phase of the cancellation signal is adjusted until it is 180 degrees out of phase with that of the clutter. Once matched up, the cancellation signal, was then modulated until its amplitude matched that of the clutter. The vector modulator used had an inherent max gain of -10 dB. If the clutter signal's amplitude was anywhere higher than that, then achieving a perfect cancellation would be impossible; however, general indications have shown that the receive antenna consistently absorbs signal at least -20 dB from that of the transmit antenna, regardless of obstructing material. This allowed for nearly 100 percent matching of the cancellation signal's amplitude with that of the clutter every test.

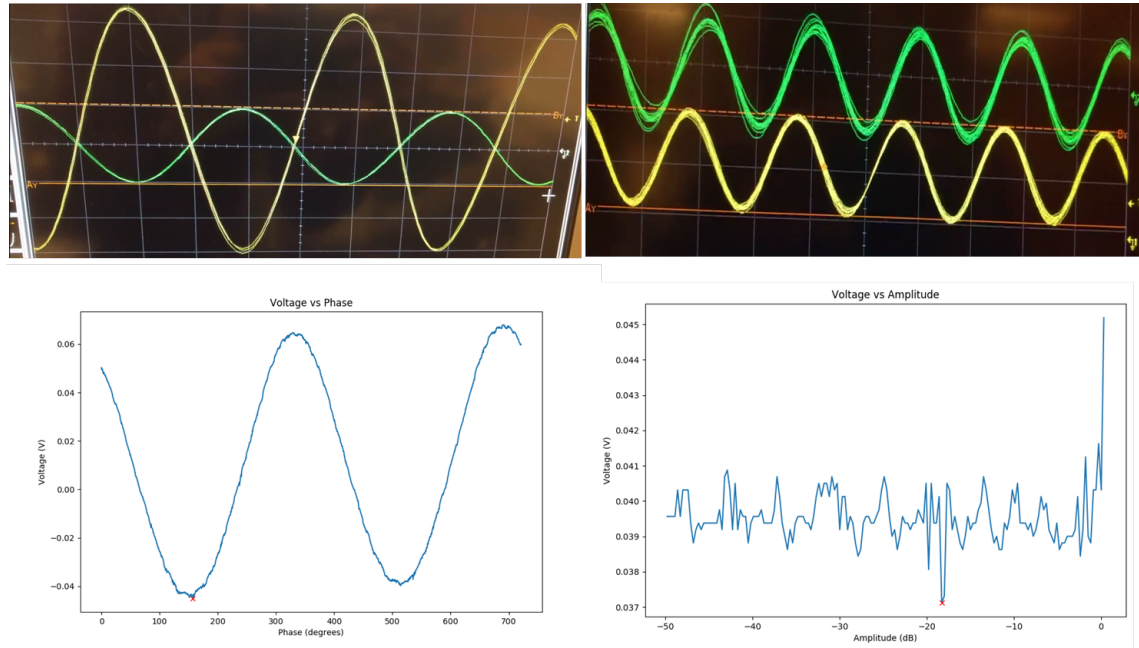


Figure 9: Tests [2]

This algorithm was verified by testing the cancellation signal's output vs the clutter signal on a 2.5 GHz spectrum analyzer. As seen in Figure 9, the first test represent a phase scan for the perfect cancellation, with the bottom right representing the mixer's output. The lowest points in the mixer output graph show perfect cancellation. On the top right graph an amplitude was also done, and at the output of the mixer an appreciable valley stood out, indicating it was at that amplitude setting that the cancellation signal matched the amplitude of the clutter.

## 5.2 Decimation

The first step in the processing method was to re-sample the entire to reduce the unnecessarily high sampling rate. The ADS 1115 has a sampling rate near 800 samples per second, and with a vital signal less than 3 Hz, there exists no need to maintain any larger frequency components within the signal. The decimation was done using a for loop that only grabbed data from the stored array list of voltage values at increments of 0.05 second increments, which would maintain a 20 Hz Sampling Rate throughout the data-set.

## 5.3 Sliding Hanning Window Buffer

After data is received from the Smoothing algorithm, it is then split into 16 discrete signals with a 60% overlap with the previous window and the next window. This is done to maximize the resolution of the signal that will be sent to the Frequency estimation algorithm. The individual windows are then multiplied by the Hanning function (shown below) to enhance the middle area of the signal. This is also done to reduce any external frequency components, or spectral leakage, that have been added to the ideal signal. The windows, multiplied by the Hanning function [11], are then sent to the filter.

$$w(n) = 0.5(1 - \cos(2\pi \frac{N}{n})), 0 \leq n \leq N \quad (4)$$

## 5.4 Filter

Each of the outputted windows by the Sliding Hanning Window Buffer are then filtered using a 2 Hz Butter-worth Low Pass filter. This was done to get rid of any residual noise residing within the 20 Hz Sampled Doppler Data. The Butter-worth had a 6th order response which allowed for a

steep cut-off at the edge of pass-band. Since this filter had a Butter-worth design, it was considered a FIR Filter, not an IIR.

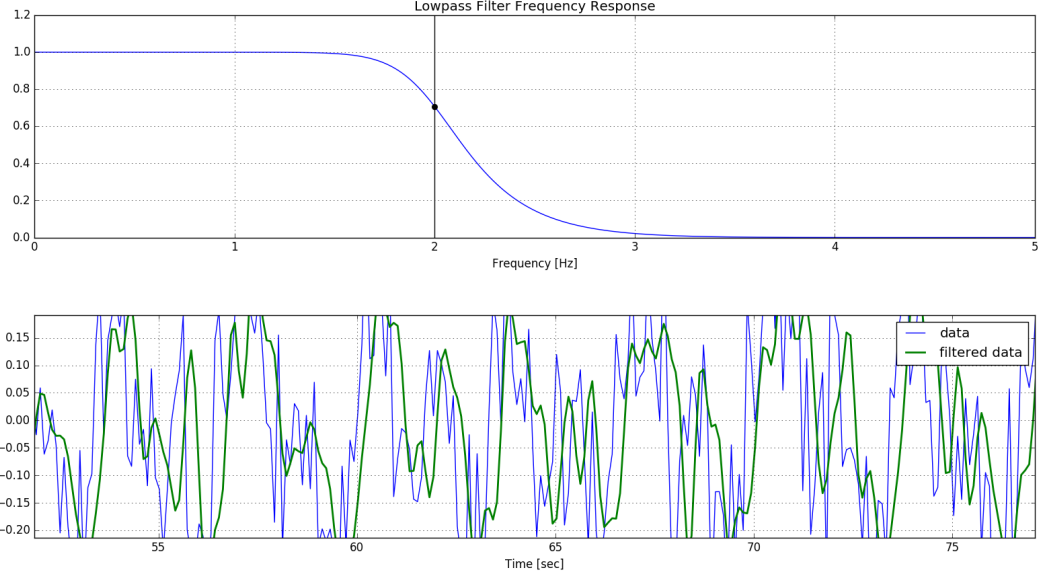


Figure 10: Low Pass Filter Response and Effect [2]

The graphs above show the effects of the low pass filter's transfer function, which essentially lets frequencies of signal less than 2 Hz Pass and greater get left out. Since this was a Butterworth filter design, with several nodes in transfer function, it is an FIR Filter not an Infinite Impulse Response (IIR) filter.

## 5.5 SNR Estimation Algorithm

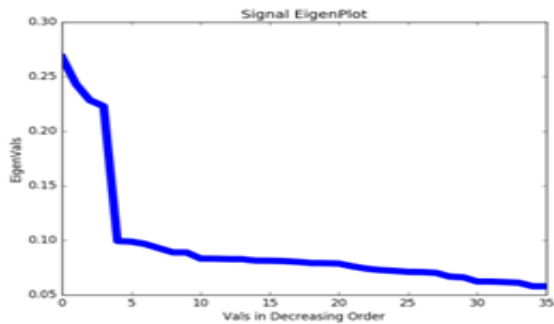
Principal Component Analysis is a statistical technique which is used to reduce the dimensionality of data. While in biological applications, it is used to reduce the number of characteristics seen by an organism, it can be used to vastly simplify the underlying structure of data in a signal processing application. First, a correlation matrix of  $n$  rows and  $m$  columns is constructed, where  $n$  represents the number of elements in the signal and  $m$  is the lag value of the matrix. The lag value is critical because it represents the number of eigenvectors generated from Singular Value Decomposition. Brute Force revealed that the approximately 36 eigenvectors were sufficient for extracting the heartbeat and respiration signals.

$$X = \begin{bmatrix} x(1) & \dots & 0 \\ \vdots & \ddots & \vdots \\ x(m+1) & \dots & x(1) \\ \vdots & \ddots & \vdots \\ x(n-m) & \dots & x(m+1) \\ \vdots & \ddots & \vdots \\ x(n) & \dots & x(n-m) \\ \vdots & \ddots & \vdots \\ 0 & \dots & x(n) \end{bmatrix}$$

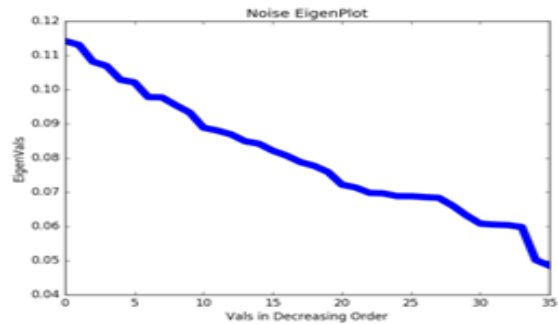
Figure 11: Correlation Matrix structure [10]

Singular Value Decomposition produces 36 eigenvectors. These eigenvectors represent the principal components in the signal, where the eigenvectors with larger magnitude are signal and eigenvectors with smaller magnitude are noise. With the underlying assumption there are only two information bearing components within the input signal, so the first two eigenvectors must have the highest magnitude, or eigenvalue. One could try to separate the signal and noise subspaces; however, in this application, an understanding of the eigenvalue plots was critical to reducing complexity of the processing application and its accuracy. The program will compute the eigenvalue plot for each of the 16 input windows. Since the signal has two information-bearing components, the first two eigenvectors must have the largest magnitude. The eigenvalue plot whose first two eigenvectors' magnitudes have the greatest summed magnitude are then selected. Going through this process selects the signal with the largest signal-to-noise ratio, devaluing the need for computing 16 Fourier Transforms and averaging the data-set, which might potentially misconstrue the true SNR Ratio within the signal. Traditional Signal-Noise-Ratios are determined by taking the ratios of dominant frequencies to noise frequencies on a frequency spectrum plot, but through the use of eigen-analysis the same statistic was capable of being generated.

As seen in Figure 14a, the eigenvalues quickly drop off with increasing numbers of eigenvectors. Only the first two eigenvalues are used in this operation, because they are indicative of the presence of a vital signal within the received Doppler data. Figure 13b is the eigenplot of a pure noise sample, which shows no steep-drop off after the first two eigenvalues and therefore, a much lower signal-to-noise ratio.



(a) Eigenplot of Signal [2]



(b) Eigenplot of Noise [2]

Figure 12: Eigenvalue plots

## 5.6 Fast Fourier Transform

The Fast Fourier Transform, or FFT, seeks to transform the Power axis into the Frequency axis by expressing every point on the original graph as a point on a sinusoid. The FFT generates sin waves that only vary in frequency for every point. It then plots the frequencies of each point's sin wave against the power axis. The resulting graph has very low frequency levels at most points, but a large spike around the "dominant frequency". A peak estimator function will locate the most dominant frequency within the observed data.

## 6 Results

### 6.1 Methodology

All tests were done under the supervision of the designated supervisor of the project. Each material tests had six trials, three trials with a human behind wall (termed signal in graphs) and three without (termed the control in graphs). Humans first signed the Human Consent Form and were given the option to opt out at any time. Subjects were then told to sit behind the wall and breathe normally for five minutes, while data was collected. Afterwards, the data was stored anonymously with only the number of the trial to ensure obscurity. The stored set was run through the Signal Processing Algorithm and the start, middle, and end versions of the data were stored in graphs. This process was repeated for each testing location.

### 6.1.1 Plaster Wall

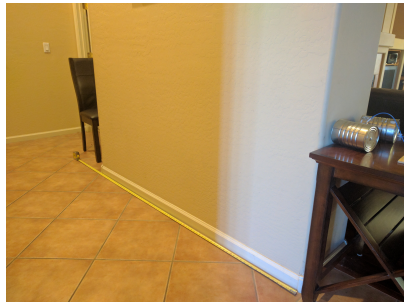


Figure 13: Plaster Test Setup

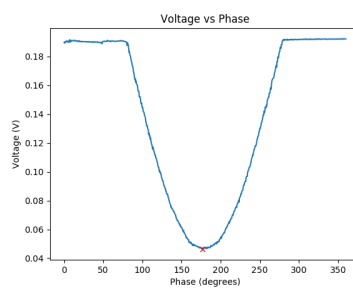


Figure 14: Phase Cali

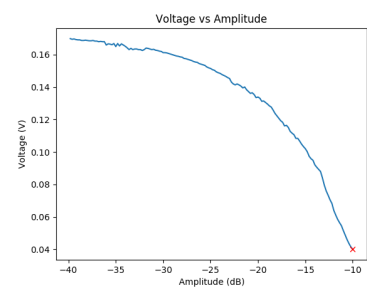


Figure 15: Amplitude Cali

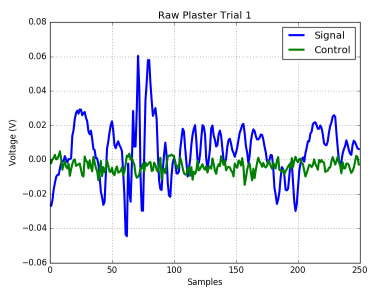


Figure 16: Raw Data 1

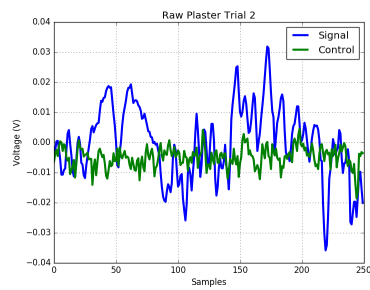


Figure 17: Raw Data 2

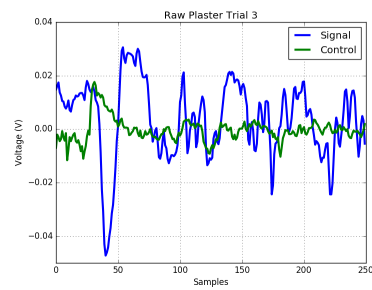


Figure 18: Raw Data 3

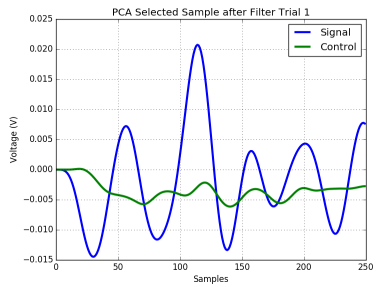


Figure 19: Processed Data 1

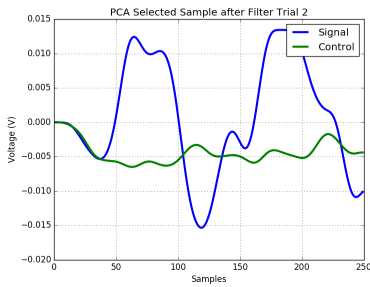


Figure 20: Processed Data 2

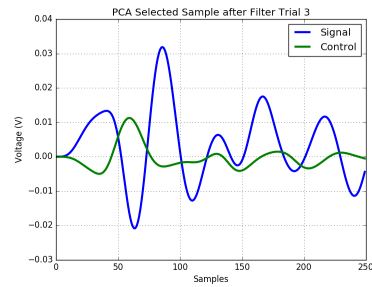


Figure 21: Processed Data 3

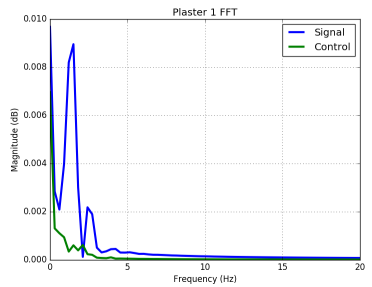


Figure 22: FFT 1

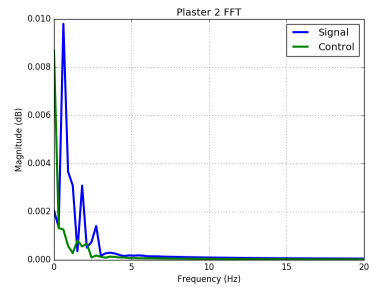


Figure 23: FFT 2

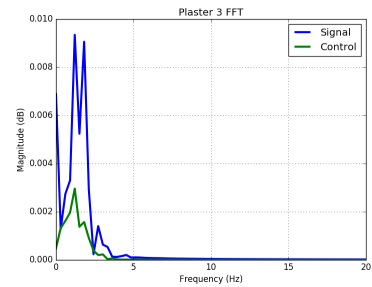


Figure 24: FFT 3

### 6.1.2 Brick Wall



Figure 25: Brick Test Setup

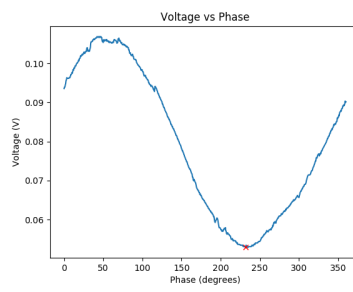


Figure 26: Phase Cali

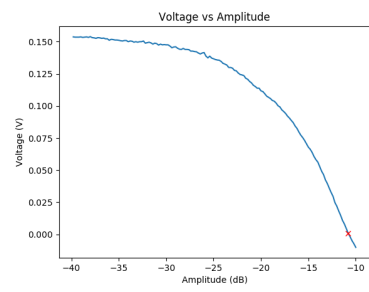


Figure 27: Amplitude Cali

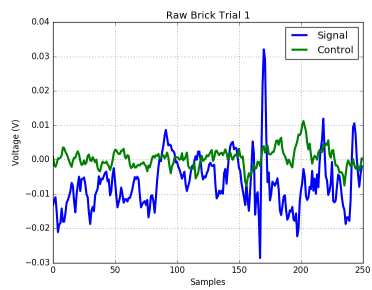


Figure 28: Raw Data 1

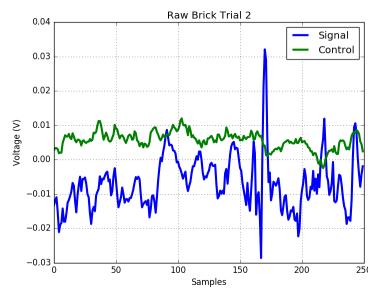


Figure 29: Raw Data 2

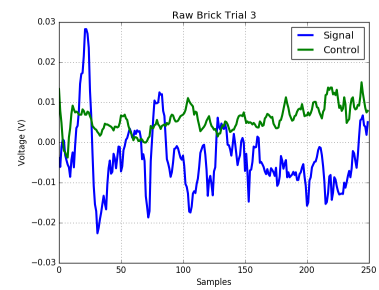


Figure 30: Raw Data 3

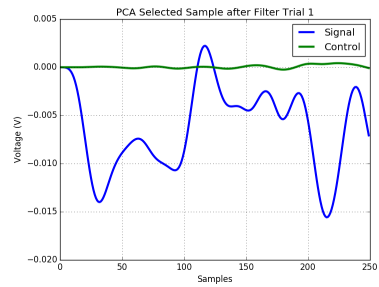


Figure 31: Processed Data 1

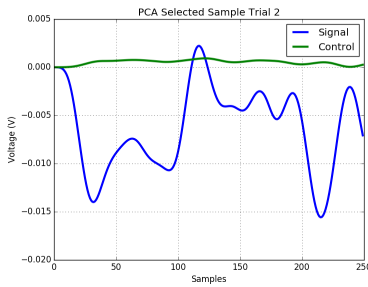


Figure 32: Processed Data 2

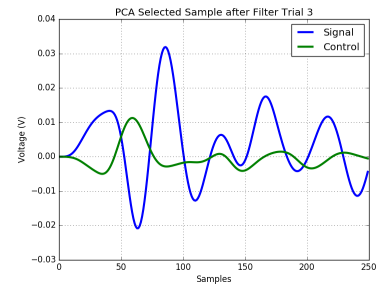


Figure 33: Processed Data 3

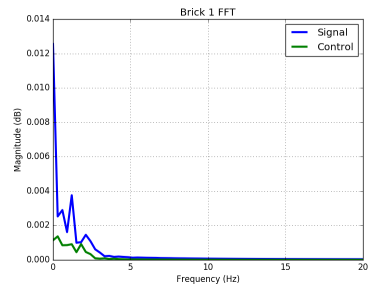


Figure 34: FFT 1

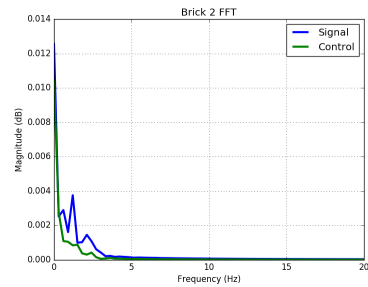


Figure 35: FFT 2

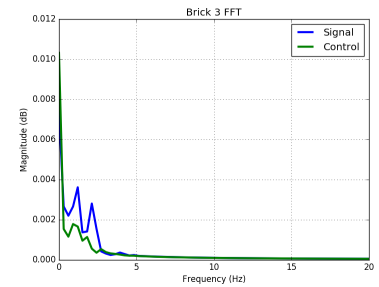


Figure 36: FFT 3

### 6.1.3 Concrete Wall

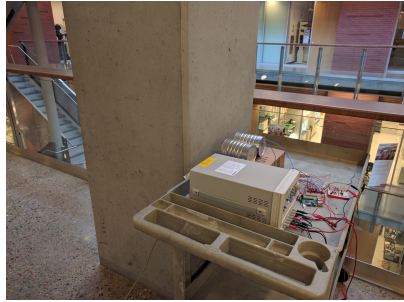


Figure 37: Concrete Test Setup

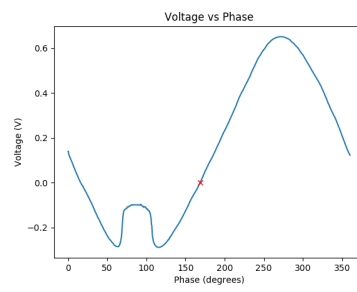


Figure 38: Phase Cali

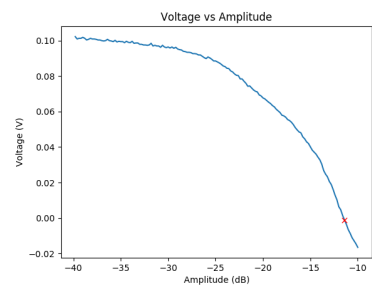


Figure 39: Amplitude Cali

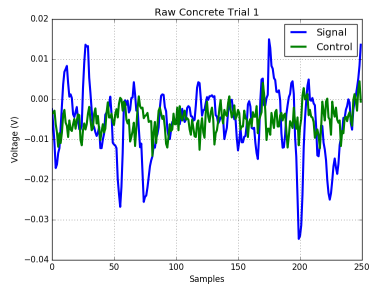


Figure 40: Raw Data 1

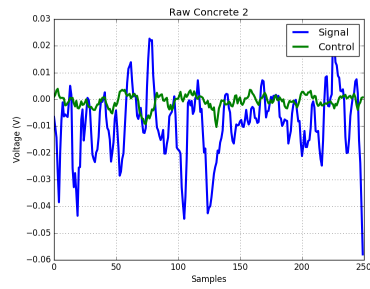


Figure 41: Raw Data 2

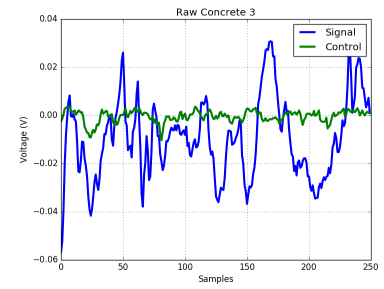


Figure 42: Raw Data 3

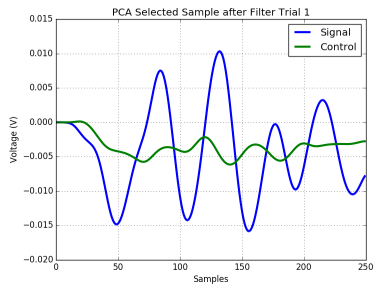


Figure 43: Processed Data 1

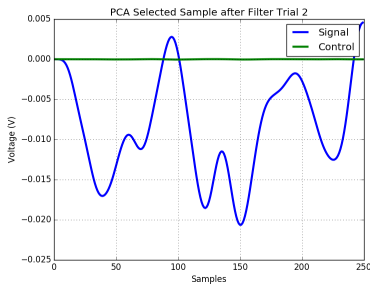


Figure 44: Processed Data 2

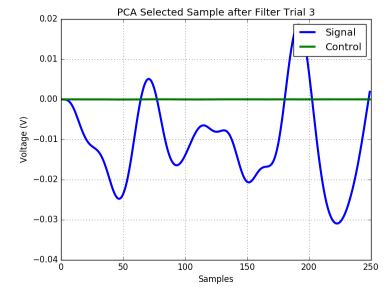


Figure 45: Processed Data 3

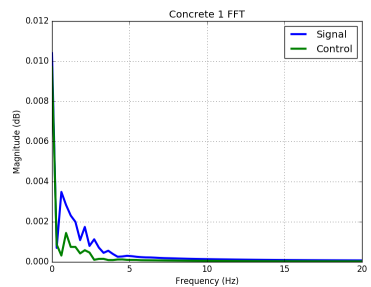


Figure 46: FFT 1

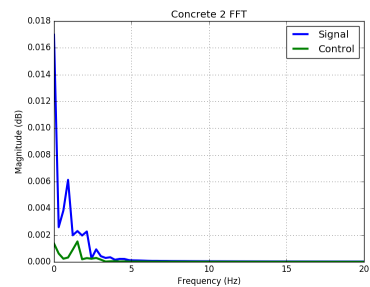


Figure 47: FFT 2

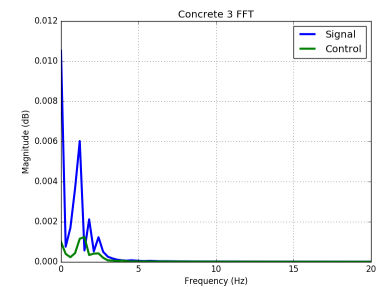


Figure 48: FFT 3

## 6.2 Analysis of Results

The materials tested upon were: 2m. of plaster, 1m. of steel-enforced concrete, and 1.5m. of brick. The plaster test was initially commenced as a proof-of-concept, to show that the proposed radar system does in fact work and can detect humans through several feet of not only plaster, but also insulation lying within the wall. By testing the radar on two varieties of thick, dense material, it was shown across the three trials that the radar was indeed capable of detecting the heartbeat and respiration signals present in the receive data. The data sampled by the ADS 1115 was quite noisy and because of its large sampling rate, contained frequency components un-necessary for vital signal detection. Therefore after processing the signals through decimation, filtering, and a sliding window buffer, the PCA selected the window which held the largest signal to noise ratio. The Fast Fourier Transforms for either data-set show strong indications of the presence of frequencies between the band of 0 - 3.3 Hz, classifying the presence of human heart and chest movements. This was further justified through observations in static control data-sets. In the voltage vs time graph for the human data-sets, voltage vs time signals oscillated between values of 0.5 and -0.5, while in the control data set values oscillated between 0.005 and - 0.005.

Also in the FFT the magnitude of spikes were much smaller and more spread out, confirming the radar's success. However, there were slight problems with the calibration sequence that must be adjusted for future use. The calibration for the brick test was flawless, but for the concrete, the otherwise clean sin-wave has a slight bump. This is attributed to the negative resolution of the ADS 1115. This chip can detect signals between -0.5 and 6.144 V, but the input signal in that regions was going below -0.5. This caused the upward bump, which is really indicative of a continuously decreasing signal in that region. Aside from the calibration process, the ratio of vital signal to noise on the Fast Fourier Transform graphs revealed a stunning relationship incurred by the current device. The sum of the powers of frequencies between 0 and 3.3 Hz divided by the sum of the powers of frequencies between 3.3 and 20 Hz was approximately 0.02 in every data-set, regardless of material. Additionally, with noise data-sets this ratio is approximately 0.005. The consistency of this ratio across materials is indicative of a binary check-mark which may be used in the future as a yes-or-no classification of whether a human is in front of the radar. If the FFT's ratio is greater than 0.02 there is a buried victim; if not, there is no victim behind the wall.

## 7 Conclusion

This project was conducted to design a clutter-cancelling Doppler radar system to detect earthquake victims buried under rubble. Last years system used a 10.525 GHz, off-the-shelf radar and some simple filtering circuitry to detect victims through air and 2 feet of cinder-block wall, which as a proof-of-concept served its purpose, but was not up to the task of true through wall detection of life. This year a radar system was built from scratch that operated at lower frequency and integrated a clutter-cancelling system. The clutter canceller consisted of a vector modulator and two digital to analog converters connected to a Raspberry PI. The calibration method designed first searched through all of phase space, for the phase of cancellation wave which would be 180 degrees out of phase with the clutter signal. Next, the system searched through all of amplitude space for the amplitude which matched that of the clutter signal. Once finished, the output of the mixer would have 0 DC offset, and the radar would commence Doppler sampling by sampling signal through a series of filters and amplifiers. The signal is stored and then processed through decimation, a sliding hanning window buffer, and filtered. There are 16 resultant windows available and in order to reduce computation and minimize the probability of muddling the output frequency spectrum, an eigen-selection algorithm the largest SNR ratio across the windows. The window with the greatest SNR was then converted to the frequency domain using the Fast Fourier Transform. Results show that the radar worked extremely well in all three cases on a brick, concrete, and plaster walls, with nine control data-sets for legitimacy. The current system is a success with strong indications of vital signals throughout trials and a threshold value was observed over all nine sets which can be used as a classifier in the future. Since the proposed system met all the design constraints initially set, this radar is a success, but needs further improvements on its implementation and testing to ensure its sure-fire viability in detecting the lives of humans.

## 8 Implementation

The finished radar was tapered to a wooden board, which with the coffee-can antennas took up a 1000000 m<sup>2</sup> area and weighed 2.8 lbs. While in remote operation at the ASU Facility, the Raspberry PI was controlled using a Python Tkinter Graphical User Interface over a Putty Client. The graphical user interface consists of several pages, where page 1 is a calibration button that must be pressed before data collection; page 2 is a data collection button that allows a user to start data collection and save a data-set to a user-specified local file, as well as the Fast Fourier Transform estimate of the signal — the FFT will pop up with a label at the top-left corner indicating whether or not a human is behind the wall according to the binary classifier ratio predicted previously; page 3 is three is a simple four channel oscilloscope measurement device, which allows the user to quickly measure the activity of each channel on the analog-digital-converter. To prevent display latency, the live graphing interface is instantiated in a separate thread.

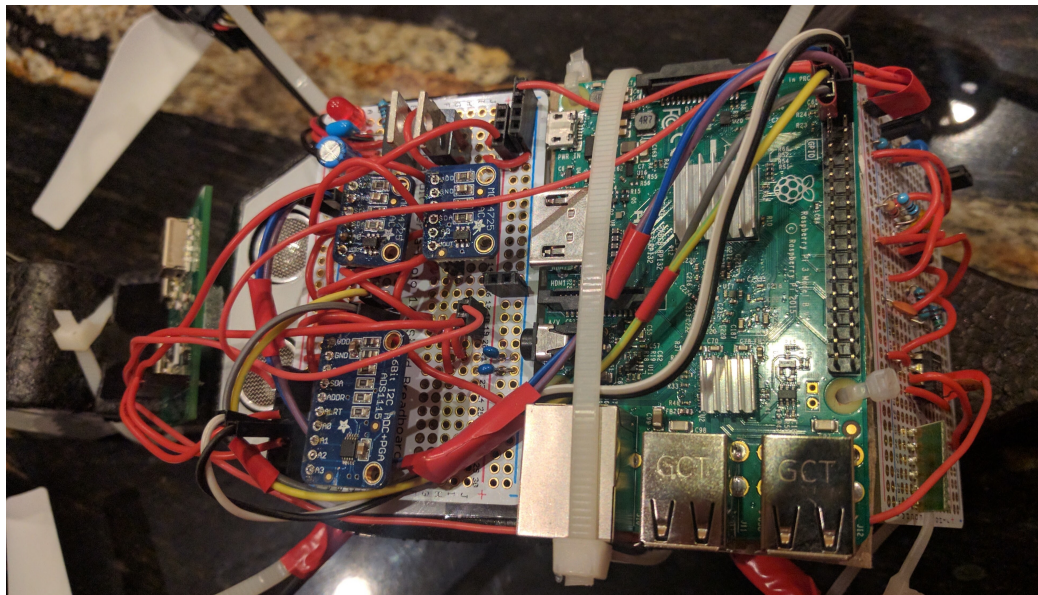


Figure 49: Parrot A.R Drone Implementation

Additionally, in order to reach full first-response efficacy, a quad-rotor implementation of the existing radar was desired. The Parrot A.R Drone 2.0 was chosen for its weight-carrying capabilities and its open source nature, allowing a first-response team to pre-plan flight plans so the drone may investigate hazardous or hostile sectors of a disaster-ridden city and store presence-of-victim data, while teams are searching easier-to-access areas. To do so, perf-board versions of the power/ADC

board and the filtering circuitry board. In order to minimize the size of the coffee-can antennas, off-the shelf 4-array patch antennas were purchased, which sported larger gains and more widespread radiation patterns in comparison to the coffee can antennas. However, it was observed that with these antennas, larger cross-sectional area came at the sacrifice of minimal increases in depth penetration.

## 9 Future Research

Future Work aims at developing a printed circuit board version of the current radar schematic to reduce cost and size. The SMA-Connected Radar's Price stems from the metal casing surrounding surface-mount chips, which are not nearly as expensive. Additionally, the most expensive component, the Vector Modulator, costs nearly 230, while the chip itself is only 14 dollars. Using a schematic drawer, a PCB Board was constructed and printed on FR-4; however, because of inconsistent dielectric constants, signal was extremely noisy and minuscule in amplitude. A new board will be printed on a Rogers Laminate.

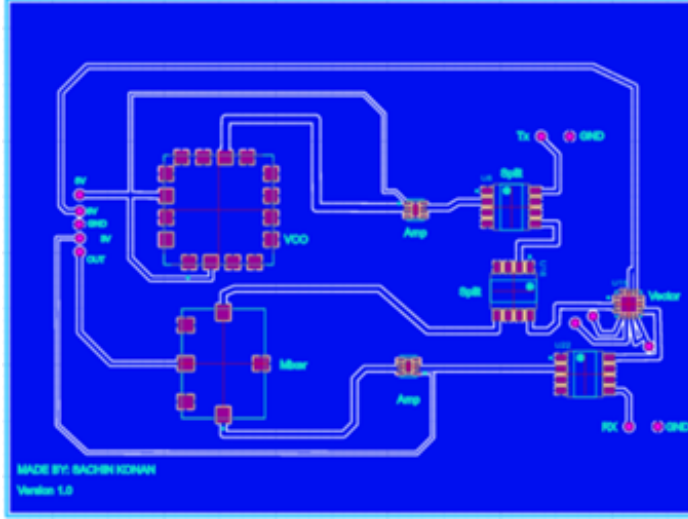


Figure 50: Printed Circuit Board Version of Doppler Radar [2]

Additionally, since the radar performed so prodigiously under the tested conditions, experiments behind larger, more dense materials may further uncover the radar's true depth penetration limit. Having an output power at the transmit antenna of nearly 27 dBm allows the radar to send out extremely high power radiation, which theoretically should be able to penetrate a maximum of 2-3

m. of brick or concrete. However, rather than perform orthodox tests against flat wall, these tests must be done on rough, non-uniform barriers to truly simulate the jagged environment affected by an environment. The multitude of frontal surfaces, gives clutter a new dimension in which the signal may not be phase or amplitude locked as in the tested scenarios.

This is where a real-time clutter cancellation system may come to fruition. During sampling of signal, a background clutter-cancellation thread will be running which will monitor time-varying DC offset shifts. If the DC value jumps, then a phase or amplitude will be adjusted. Since phase generally doesn't change with time (in the scope of a trial), a probabilistic amplitude varying thread may run to minimize an oscillating DC-offset.

## References

- [1] Equation made by students. .
- [2] Picture taken by students. .
- [3] Y. Douglas. Challenges of the modern fireground, May 2016.
- [4] A. girl Chapfuwa. Radar signal processing for stand-off life sign monitoring. Department of Electrical and Computer Engineering.
- [5] A. Høst-Madsen, N. Petrochilos, O. Boric-Lubecke1, V. M. Lubecke, B.-K. Park, and Q. Zhou. Signal processing methods for doppler radar heart rate monitoring. *Kai Sensors, Inc*, 2010.
- [6] B. Jang, S.-H. Wi, J.-G. Yook, M.-Q. Lee, and K.-J. Lee. Wireless bio-radar sensor for heartbeat and respiration detection. *Progress In Electromagnetics Research*, 5:149–168, 2008.
- [7] D. Jenn. Radar fundamentals, April 2007.
- [8] D. C. D. N. Kedar Nath Sahu and D. K. J. Sankar. Study of rf propagation losses in homogeneous brick and concrete walls using analytical frequency dependent models. *R Journal of Electronics and Communication Engineering*, 5:2278–2834, 2014.
- [9] H. D. Khunti. Researcher. Masters of science thesis, Arizona State University, August 2013.

- [10] MathWorks. Data matrix for autocorrelation matrix estimation, . URL <http://www.mathworks.com/help/signal/ref/corrmtx.html>. [Online; accessed September 14, 2016].
- [11] MathWorks. Hann (hanning) window, . URL <http://www.mathworks.com/help/signal/ref/hann.html>. [Online; accessed September 8, 2016].
- [12] M. Z. G. N. and M. Badnerkar. A modern microwave life detection system for human being buried under rubble. *International Journal of Advanced Engineering Research and Studies*, 1 (1):69–77, 2012.
- [13] B. Stevens. Platypus. Internet, August 2014.

## Resources

The electrical and Python Code are Open-Source and can be found at the github link. Under the electrical tab, the LTSpice Simulations for the Filter/Amplifier Circuit can be found. Under the main tab, the Python program called realmain.py is the code that controls the raspberry pi and the clutter cancellation system. The rest of the folders are individual testing beds for the elements in the realmain.py code. Additionally, the Simulations tab contains radar simulations for observing the clutter and its affect on the DC offset.

<https://github.com/SachinKonan/DopplerLifeDetectionSystem>